A combination of fourier transform and machine learning for fault detection and diagnosis of induction motors

Nguyen, D.V.; Zwanenburg, E.; Limmer, S.; Luijben, W.; Bäck, T.H.W.; Olhofer, M.

A Combination of Fourier Transform and Machine Learning for Fault Detection and Diagnosis of Induction Motors

2021 8th International Conference on Dependable Systems and Their Applications (DSA) | 978-1-6654-4391-3/21/$31.00 ©2021 IEEE | DOI: 10.1109/DSA52907.2021.00053

Van Duc Nguyen
Leiden Institute of Advanced Computer Science
Leiden University
Leiden, The Netherlands
vdnguyen77@gmail.com

Ewout Zwanenburg
Leiden Institute of Advanced Computer Science
Leiden University
Leiden, The Netherlands
ewout.zwanenburg@gmail.com

Steffen Limmer
Honda Research Institute Europe GmbH
Offenbach am Main, Germany
steffen.limmer@honda-ri.de

Wessel Luijben
Samotics Company
Leiden, The Netherlands
wesselluijben@semioticlabs.com

Thomas Bäck
Leiden Institute of Advanced Computer Science
Leiden University
Leiden, The Netherlands
T.H.W.Baeck@liacs.leidenuniv.nl

Markus Olhofer
Honda Research Institute Europe GmbH
Offenbach am Main, Germany
Markus.Olhofer@honda-ri.de

***Abstract*—Induction motors are widely used in different indus-try areas and can experience various kinds of faults in stators and rotors. In general, fault detection and diagnosis techniques for induction motors can be supervised by measuring quantities such as noise, vibration, and temperature. The installation of mechanical sensors in order to assess the health conditions of a machine is typically only done for expensive or load-critical machines, where the high cost of a continuous monitoring system can be justified. Nevertheless, induced current monitoring can be implemented inexpensively on machines with arbitrary sizes by using current transformers. In this regard, effective and low-cost fault detection techniques can be implemented, hence reducing the maintenance and downtime costs of motors. In this work, machine learning techniques have been combined with traditional Fast Fourier Transform (FFT) to proposes a simple but yet efficient method for fault detection and diagnosis of induction motors. Raw signals are converted from time domain to frequency domain using FFT. The FFT spectrum are then divided into frequency segments and energy coefficients of each segment are calculated as the sum over the FFT amplitudes. These energy coefficients are used as features for machine learning in our platform. The proposed method is validated on real-world data and achieves a precision of 99.7% for fault detection and 100% for fault classification with minimal expert knowledge requirement. In addition, this approach allows users to be able to optimize/balance risks and maintenance costs to achieve the highest benefit based on their requirements. These are the key requirements of a robust prognostics and health management system.**

This work is part of the research programme Smart Industry SI2016 with project name CIMPLO and project number 15465, which is partly financed by the Netherlands Organisation for Scientific Research (NWO). We acknowledge Samotics Company for providing us the data and fruitful discussions.

Keywords: Fault detection, Fourier Transform, induction motor, predictive maintenance.

I. Introduction

A. Induction motor and its main defects

Induction motors are widely used in industrial drives because they are rugged, reliable, and economical [1]. They became an industry workhorse and play a pivotal role in industry for conversion of electrical into mechanical energy. In order to improve electric motor efficiency, variable speed drives are commonly used, and this has led to increased motor overheating problems, harmonic problems, and shorter operational life of motors.

In general, faults that may occur in an induction motor can be classified into four groups namely bearing faults, stator faults, rotor faults, and other faults [2]. Statistical studies of IEEE [3] show that bearing faults are the most frequent faults in electrical motors (42%), followed by stator (28%) and rotor (8%) faults. The rest (22%) are other faults. A bearing comprises an outer ring, an inner ring, and a set of rolling elements, called balls, which are placed in raceways, which are spinning inside the rings. Fatigue failures may be caused due to the continual stress on these bearings. Whenever there is a failure in a bearing it results in certain vibrations, which influences the eccentricity in the air gap between the rotor and stator and increases the noise levels. Improper insulation, corrosion, contamination, improper lubrication are also responsible for bearing failures. Stator faults cover short circuit, loss of supply phase, etc. The winding faults associated

978-1-6654-4391-3/21/$31.00 ©2021 IEEE
DOI 10.1109/DSA52907.2021.00053

with stator winding are often caused by a failure of insulation of winding, which leads to local heating. If unnoticed, this local heating further damages the insulation of stator winding till catastrophic failure occurs [4]. Rotor faults consist of coupling error, broken bar, broken end-ring, etc. There are numerous reasons for faults in the rotor of an induction machine that include thermal stresses, magnetic stresses, dynamic stresses, mechanical stresses, and environmental stresses [5]. Additionally, faults in the cage of the rotor are more prevalent for medium voltage motors than for motors of small size due to higher thermal stress in the rotor of the machine. Other faults include (but are not limited to) static, dynamic, and mixed air-gap eccentricities. Eccentricity arises due to non-uniform air-gap amidst the stator and rotor [5], [6]. This may be generated by bearing defects or manufacturing failures. Extreme air gap eccentricity may commence inequitable radial forces and finally result in friction between stator and rotor, which may lead to severe damage to the core of the stator and rotor, further causing a breakdown of the motor.

B. Review of motor fault detection and diagnostics methods

A fault in an induction motor may result in idle times, for example, in a production pipeline, and hence in losses of revenue. In order to decrease the downtime and to ensure reliable and safe operation, fault recognition in an early stage is desirable, which necessitates condition-based monitoring of the induction motor. Classical condition monitoring methods using mechanical quantities such as vibration, torque, noise, acoustic signals, and temperature are well researched and presented. However, whenever mechanical sensors are used to assess the health conditions of a machine, they are installed on some expensive or load-critical machines where the high cost of a continuous monitoring system can be justified [7]–[9]. Moreover, the implementation of these measuring systems proves to be only suitable in the case of large motors or critical applications. Readers who are interested in condition monitoring methods using mechanical quantities can find more information in these papers [2], [7], [9].

To overcome the above-mentioned drawbacks, researchers have been using Motor Current Signature Analysis (MCSA) for condition monitoring. The biggest challenge of a MCSA technique is that incipient fault signatures are inherently weak and susceptive to attenuation and thereby can be buried in signal noise [10]–[13]. The most popular techniques under MCSA are current signature analysis, voltage signature analysis, extended Park's vector approach, Wavelet Packet, Hilbert transform, Hidden Markov Models, and instantaneous power signature analysis [2], [13]–[20]. These physics-based models are complex and require prior knowledge of the induction motor system as well as a detailed description of the technical parameters of the motor. Due to the complexity of induction motors, in which mechanical, electromagnetic, or electromechanical effects are often coexistent, the specific prior knowledge of fault mechanism and corresponding reflections on measured sensor data becomes elusive with respect to arbitrary application scenarios [21]. In addition, these techniques require human interpretation, which is not preferable in the real-world applications [2], [13], [22], [23].

With the rapid development of artificial intelligence (AI), automated fault diagnostic systems using data-driven models have been becoming a new trend for condition monitoring of induction motors in particular as well as in prognostics and health management (PHM) systems in industry in general. Recently, there have been some applications of various data-driven models for motor fault detection and diagnosis problems. Most of these works relied on (deep convolution/artificial) neural networks that require large (labeled) training datasets and have a high computational complexity [9], [22], [24]–[31]. Support vector machine (SVM) models [32]–[35], statistical processing, k-Nearest Neighbour [34], dictionary learning and Nystrom [21], and hybrid fuzzy min-max [9] were also used. However, those benchmarks were validated either on simulation or lab/experimental data, which is recorded under well-controlled conditions. Nonetheless, in the industry/real-world, induction motors are required to operate in highly corrosive and dusty environments which causes a lot of noise [36]. Application on real-world data might be limited because the accuracy of the models often reduces significantly with noise [9].

This paper proposes a low-cost, elegant, and yet accurate approach for fault detection and diagnosis of induction motors based on using stator current. This approach uses traditional/classical Fast Fourier Transform and modern/advanced machine learning techniques and does not require any domain/expert knowledge as well as technical parameters of the motor. In addition, our benchmark allows users to be able to adjust risks and maintenance costs to gain the best benefit based on their requirements. These are the key requirements of a robust prognostics and health management system. The proposed approach was validated on real-world data with three different health conditions and demonstrated high precision compared to the existing methods. The best classifier achieved overall classification precision of 99.7% for fault detection and 100% for fault classification.

The rest of this article is organized as follows: Section

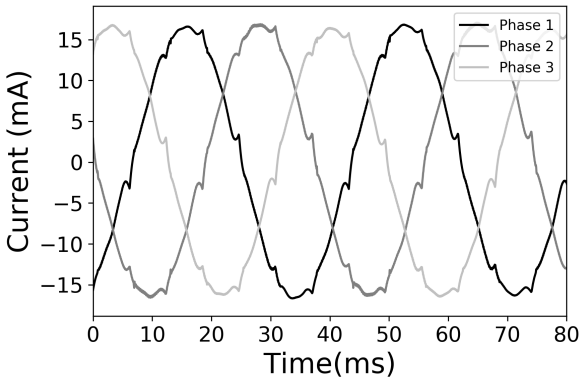

Fig. 1. An example of the three-phase stator current.

II provides detailed information on the data used in the experiments. Section III describes the data preprocessing steps and our methodology. In Section IV, we report and discuss the "experimental" results. Finally, a conclusion is provided in Section V.

II. Dataset description

Data of two induction motors, which are in real working conditions, was provided by Samotics Company [37], the Netherlands. The configurations of the two motors are different and their technical details are described in Table I. All three phases of stator current were collected under full load conditions and with a grid frequency of 50 Hz. The recording duration of each measurement is 15 seconds with a sampling rate of 20 kHz. An example window of all three phases in the real-time of the stator current is shown in Fig. 1. All three phases are periodic and include noise.

The data set contains measurements of the motors in three different conditions: healthy, coupling fault, and bearing fault. The total number of measurements corresponding to each condition of each motor is shown in Table II. The actual health states were determined by experts in the field.

III. Methodology

A. Fast Fourier Transform and pre-whitening

To analyze the periodic signal, among many signal processing techniques used in the literature, Fast Fourier Transform (FFT) is one of the most popular ones. FFT converts a signal from its original domain (often time or space) to a representation in a frequency domain. We use FFT as the first step for condition monitoring and fault diagnosis because it relies on the variations in the frequency to isolate various faulty conditions. There are three phases of the stator current and we use mean FFT results for our analysis. The mean FFT is achieved by taking an average FFT of all three phases of each measurement.

TABLE I
Main technical parameters of two motors

Parameters	**Motor I**	**Motor II**
Motor type	160MA	180MA
Number of poles	4	2
Rotation speed	1470 rpm	2950 rpm
Main frequency	50 Hz	50 Hz
Efficiency	0.914	0.927
Power factor	0.86	0.9
Power	11 kW	22 kW
Shaft diameter	32 mm	24 mm
Coupling type	Standard	Spacer
Gross weight	351 kg	280 kg

TABLE II
Number of measurements per motor and health state

Motor	**Healthy**	**Bearing**	**Coupling**
Motor I	1343	2291	54
Motor II	374	3241	18

The most common limitation of the FFT technique is its application to noisy signals. To overcome this issue, a pre-whitening method is normally applied [38], [39]. In this work, the pre-whitening operation was done by normalizing the spectrogram by its average value taken over 10 frames. This is supposed to remove the constant baseline endured all along with the operation, which includes structural resonances of the system as well as of the machinery. After pre-whitening, if the signal is stationary the spectrogram is supposed to be completely white. This operation has been found important to better enhance the contrast between the beginning and the end of the test. These step helps us to better enhance the contrast between the beginning and the end of the system operation as well as the magnitude of the noises.

B. Platform for Machine Learning

A first and important step in machine learning is to produce and extract relevant features. We took the advantage of the FFT spectrum of the stator current to create features by following the work of [40]. The FFT spectrum is divided into different frequency segments. Explicitly, for frequencies up to 2000 Hz, the main peak segments were created in a way that the center of each segment was the harmonic order of the fundamental frequency (50 Hz) with a bandwidth of 20 Hz. This results in eighty-two segments in total. The first 10 main-peak, and off-peak segments are shown in Fig. 3. Next, the energy coefficients of each segment were calculated as the sum over the FFT amplitudes. These energy coefficients were used as features for machine learning in our platform. All features were re-scaled to have a scale from zero to one by using Max-Min normalization before feeding them to any machine learning model.

Five common algorithms for binary classification including K-nearest neighbor (KNN), Decision Tree (DT), Random Forest(RF), Logistic Regression (LG), and Support Vector Machine (SVM) were used. Grid search with a repeated stratified k-fold cross-validation method was used to tune the hyperparameters of the employed models. The dataset was stratified, meaning that each fold of the cross-validation split would have the same class distribution as the original dataset. The random seed was fixed to achieve a reproducible result.

In the case of balanced datasets, a repeated stratified 10-fold cross-validation was used for hyperparameter tuning. For this experiment, we evaluated the model's performance on accuracy, precision, recall, f1 score, and false negative number.

In the case of severely imbalanced datasets, a repeated stratified 5-fold cross-validation was used. For each fold, the test set was kept unchanged while the train set was treated using two approaches: Synthetic Minority Oversampling Technique (SMOTE) for the minority class, and a combination of under-sampling technique for the majority class and SMOTE for the minority class. In general, SMOTE creates extra training data for the minority class by synthesizing new samples based on real data. More specifically, the minority class is over-sampled by taking each minority class instance and introducing synthetic instances along the line segments joining any/all

of the k minority class nearest neighbors. Depending upon the amount of over-sampling required, neighbors from the k nearest neighbors are randomly chosen. This procedure can be used to create as many synthetic instances for the minority class as are required. The approach is effective because new synthetic instances from the minority class are created that are plausible and relatively close in feature space to existing instances from the minority class [41], [42]. On the other hand, the under-sampling of the majority class was performed by randomly picking samples without replacement from the original data.

In the class imbalanced case, it is widely admitted that accuracy tends to give a deceptive evaluation for the performance [43], [44]. Instead of accuracy, the Area Under the ROC Curve (AUC), and Geometric Mean (GM) are the most commonly used performance metrics in the imbalanced learning domain [45]. In this study, for severely imbalanced datasets, AUC and GM were used as the performance evaluation metric,

$$AUC = \frac{1 + TP_{rate} - FP_{rate}}{2}, \tag{1}$$

$$GM = \sqrt{TP_{rate} \times TN_{rate}}, \tag{2}$$

where true positive rate, $TP_{rate} = \frac{TP}{TP+FN}$, is the percentage of positive instances correctly classified. True negative rate, $TN_{rate} = \frac{TN}{TN+FP}$, is the percentage of negative instances correctly classified. And false positive rate, $FP_{rate} = \frac{FP}{FP+TN}$, is the percentage of negative instances misclassified. Here *TP*, *TN*, *FP*, and *FN* indicates the number of true positives, true negatives, false positives, and false negatives, respectively.

IV. Results and Discussions

A. Fast Fourier Transform and pre-whitening

An average FFT over three phases of a healthy motor (motor type I) at 50 Hz is shown in Fig. 2. In this illustration, the odd (*O*) fundamental frequency components are barely pronounced while the even (*E*) ones are very fuzzy. It is in a good agreement with three-phase circuit theory [10].

Additionally, we observed many other frequency components (*N*) with magnitudes that are comparable to the harmonics of the fundamental. The apparent of the these components might be due to the following reasons: (i) the rotor of an induction machine rotates at a frequency that is different from the electrical supply frequency and this difference in speed is directly proportional to (and fluctuates with) the load level, (ii) cyclical load torque variation, (iii) eccentricities and inherent mechanical asymmetries, (iv) air-gap permeance, (v) mechanical misalignment, and (vi) random noises [10]. The mechanical misalignment issue is the most common cause. When a machine is directly coupled to a load, exact alignment of the two shafts is difficult. Any amount of misalignment will contribute to an eccentricity and a position dependent load torque variation as well. From now on, we will call these frequency components 'random noises'. Mechanical misalignment and noises are very common in industry and lead to a big challenge for condition monitoring. A comparison of a full FFT spectrum of healthy-, bearing fault- and coupling fault motors is shown in Fig. 3. We can hardly distinguish the spectra by the naked eyes.

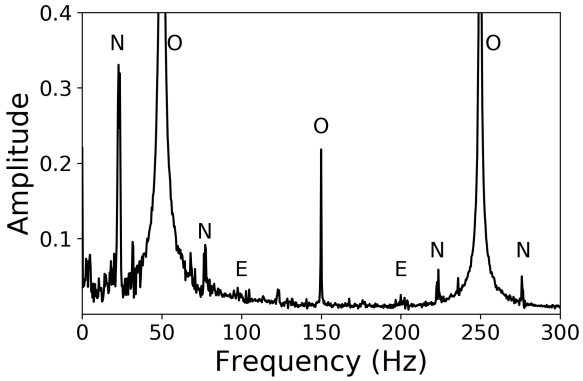

Fig. 2. Fast Fourier Transform spectrum of a healthy motor; An *O* indicates an odd harmonic, an *E* indicates an even harmonic, and an *N* indicates random noise.

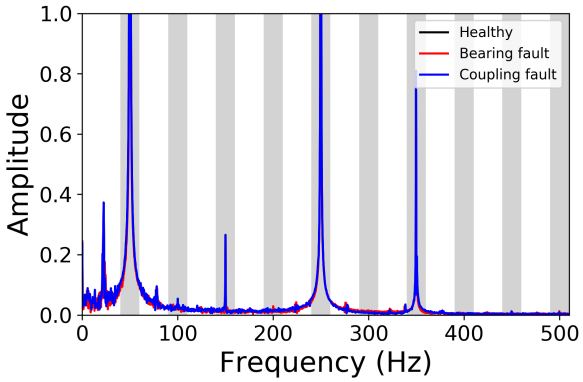

Fig. 3. A comparison of FFT spectrum and energy calculation of healthy-, bearing fault- and coupling fault motors. Gray- and white windows are main-peak-, and off-peak segments, respectively.

To provide an overview of the FFT spectrum and magnitude of noises over time we show pre-whitening results in Fig. 4. This plot shows the first fifty cycles/measurements of the pre-whitened spectrogram of motor **I** and all motor conditions. In all cases, including the healthy motor, the spectrograms are not completely white. This indicates that the stator current is not stationary. The instability of the signal is more pronounced at the fundamental harmonics. We attribute this instability to mechanical misalignment and random noises which we have mentioned above. More importantly, we can not classify conditions of the motor based on these pre-whitened spectrogram.

B. Fault diagnosis

The main tasks of fault diagnosis are fault detection, fault classification, fault location, fault recovery and so on. As soon as the fault is detected, the fault category then needs to be identified. Fault classification is to determine which kind of fault has occurred, that is so to say, to distinguish the causes

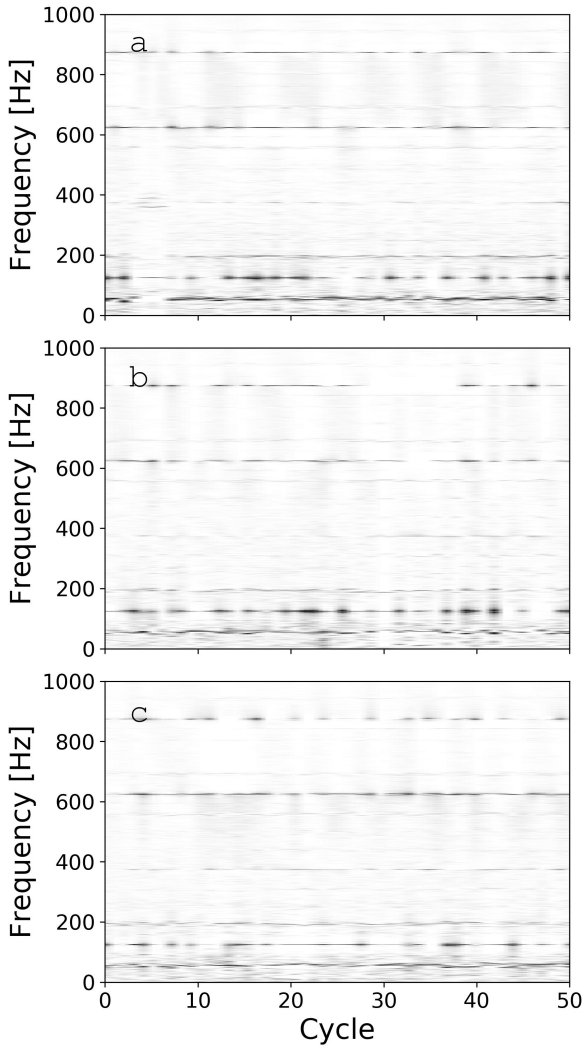

Fig. 4. Pre-whitening spectrogram of: healthy- (a), bearing-defect- (b), and coupling-defect motors (c)

of the observed abnormal conditions. Once the fault category is determined, the corresponding troubleshooting measures will be taken immediately. This timely troubleshooting may avoid greater economic losses and casualties [46]. Our fault diagnosis platform was divided into two steps; fault detection, and fault classification. The main task of the first step is to distinguish the unhealthy motors from the healthy ones. In the second step, bearing fault and coupling fault are distinguished. In the real-world application, the first step is more important for safety while the second one helps to reduce the maintenance costs and time. For the fault diagnosting and classification, we used the approach based on FFT and machine learning as described in Section III-B.

1) Fault detection: As mentioned before, the dataset contains data from two motors. For the fault detection step, the bearing-fault and coupling-fault states/classes were combined to an unhealthy state/class. In total, there were 1717 healthy and 5604 unhealthy samples in the aggregated dataset. The

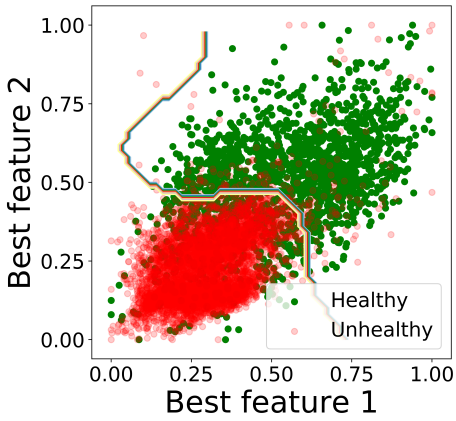

Fig. 5. Decision boundary (solid line) of SVM classifier between healthy (green) and unhealthy (red) samples.

dataset was then split into train- and test sets with a ratio of 70% and 30%, respectively. This results in a test dataset size of 1831 observations, which include 441 healthy and 1390 unhealthy samples.

Evaluation scores on the test data of the five algorithms are reported in Table III. The table is sorted in an increasing order of precision. All five models show very high precision with a minimum precision of 97.7%. Furthermore, with a precision and recall of 99.7%, SVM outperforms the other classifiers. It is higher than the scores achieved on lab data in previous work [22], [29], [32], [35]. In addition, besides the highest precision, SVM also shows less computational costs. The outperformance of SVM is in a good agreement with the earlier reports since SVM is the most efficient classification method for binary classifying [32], [35], [46]. A visualization of the two classes on the two best out of the 82 features space and the decision boundary of the best model is shown in Fig. 5. Where feature ranking was performed based on the random forests classifier.

To prove that our models were not over-fitted, we used the following methods: i) using k-fold cross validation to validate our models on different test datasets, ii) splitting the data into train- and test sets by time. In all cases we achieved more or less the same scores as reported in table III.

Regardless of the high precision, for a number of samples the prediction was false negative (FN). A false negative means, the model indicates the motor is healthy but in fact it is unhealthy. False negative is normally dangerous in the real-world application and needs to be minimized. An effective PHM system, however, should allow practitioners to flexibly balance between the safety and the operation and maintenance costs to achieve the desired trade-off. Whether the prediction accuracy is good enough for the real-world application depends very much on the industry. For example, in the nuclear and aerospace industries, the safety requirements are high, hence the achieved accuracy might not meet the requirements. However, in other industries where multiple machines operate in a parallel system (e.g., many pumps in a pump system),

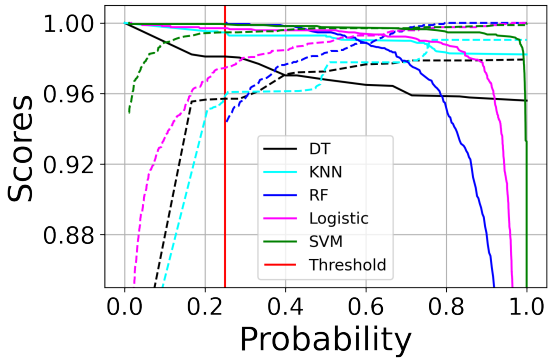

Fig. 6. Precision (dashed line) and recall (solid line) vs. prediction probability. The vertical red line shows the threshold in which the FN of the best model equals zero.

TABLE III
Evaluation scores of fault detection; f1 score (f1), precision, recall, and false negative number (FN) of all classifiers. The table is sorted in an increasing order of precision.

Classifiers	f1	Precision	Recall	FN
DT	0.971	0.977	0.965	59
KNN	0.984	0.978	0.99	17
RF	0.989	0.984	0.995	9
Log	0.993	0.989	0.996	7
SVM	0.997	0.997	0.997	5

operators might accept high risk in order to reduce unnecessary maintenance and overall costs. For such industries, the prediction precision is certainly high enough. Additionally, in the real-world application, users prefer to have a flexible platform where they can decide themselves the risk they would take and the maintenance costs in order to gain the best benefit. We fulfill this requirement by proposing a method to tune the number of false negatives and precision. Practically, we used predict-probability function from Scikit-learn to achieve the raw probability that a sample was predicted to be in either a healthy or unhealthy class. Then a trade-off for the false negative rate and the model accuracy was realized by tuning the threshold of the prediction probability for the positive class. In general, lowering the value of the threshold leads to a decrease of precision, however, it allows us to increase the recall score and to reduce the number of FN values. We were able to achieve zero FN which corresponds to a recall of 100% with the RF model at a threshold of 0.25 (vertical red line) while keeping a high precision of 94.4%. Precision and recall scores versus prediction probability are shown in Fig. 6.

2) Fault classification: The second step of our platform is to classify the type of defect in the motor. In this step, bearing faults and coupling faults are distinguished. There are 72 coupling fault and 5532 bearing fault samples in the dataset. Thus, there is a great imbalance between the two classes due to the fact that a pump coupling defect often leads to severe damage and needs immediate action. In contrast, bearing defects are normally fuzzy and immediate action is

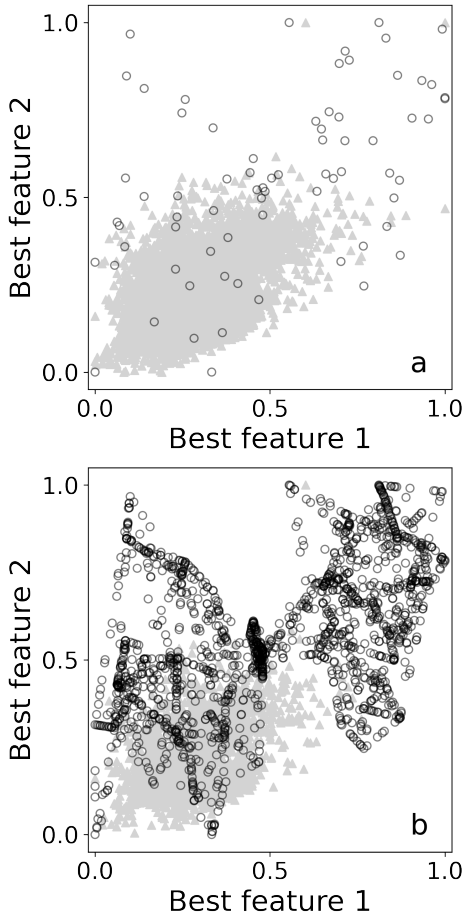

Fig. 7. A visualization of the bearing defects (solid gray triangles) and coupling defects (open black circles) on the feature space: original dataset (a), and the data set after balancing by combining SMOTE and undersampling (b).

not urgently necessary. In this experiment, repeated stratified 5-fold cross-validation method was used. For each fold, the test set was kept unchanged while the train set was treated using two resampling techniques including Synthetic Minority Oversampling Technique (SMOTE) for the minority class, and a combination of under-sampling technique for the majority class and SMOTE for the minority class. The under-sampling of the majority class was performed with an under-sampling strategy of 50% of the original data while the over-sampling of the minority class was executed with the number of nearest neighbors equal to five. A visualization of the bearing defect and coupling defect samples of the train data set as original and after balancing by combining SMOTE and undersampling is shown in Fig. 7. A comparison of the performance metrics (GM and AUC) of the five above mentioned classifiers of the two resampling techniques with the original data is shown in Table IV. We observed a significant improvement of all algorithms after the class balancing. More importantly, all classifiers show reasonably high Area Under the ROC Curve (AUC), and Geometric Mean (GM). Especially, with the SVM

TABLE IV

Area Under the ROC Curve (AUC), and Geometric Mean (GM) scores of bearing- and coupling defect classification with three resampling methods. The table is sorted in an increasing order of GM for the combination resampling technique.

Classifiers	**No-resampling**		**SMOTE**		**Combination**	
	GM	AUC	GM	AUC	GM	AUC
DT	0.751	0.779	0.848	0.859	0.808	0.827
RF	0.684	0.982	0.798	0.991	0.864	0.988
KNN	0.627	0.862	0.875	0.910	0.874	0.937
Log	0.745	0.968	0.944	0.990	0.927	0.990
SVM	0.887	0.994	0.928	0.995	0.937	0.995

classifier, we achieved a value of 0.995 and 0.937 for AUC and GM, respectively.

V. Conclusions

This paper proposes a low cost, but yet accurate and robust fault diagnosis method for induction motors based on stator current signal. The proposed approach is built by combining Fast Fourier Transform and machine learning algorithms. Our method was validated on real-world data with three different health conditions and demonstrated high precision compared to the existing methods. The best classifier achieved overall classification precision of 99.7% for fault detection and AUC of 99.5% for fault classification. In addition, our platform allows users/practitioners to adjust between risk and maintenance costs in order to achieve the best benefit. This is a key mission of a robust prognostics and health management system. It is worth to mention that our approach was constructed without any requirement of deep domain knowledge of induction motor as well as any technical/mechanical parameter. Therefore, the proposed approach is expected to be a universal and generic solution for all rotating machinery.

References

[1] D. Siyambalapitiya and P. Mclaren, "Reliability improvement and economic benefits of on-line monitoring systems for large induction machines," *IEEE Trans. Ind. Appl.*, vol. 26, pp. 1018 – 1025, 1990.

[2] S. Kumar, D. Mukherjee, P. K. Guchhait, R. Banerjee, A. K. Srivastava, D. N. Vishwakarma, and R. K. Saket, "A Comprehensive Review of Condition Based Prognostic Maintenance (CBPM) for Induction Motor," *IEEE Access*, vol. 7, pp. 90 690–90 704, 2019. [Online]. Available: https://ieeexplore.ieee.org/document/8754739/

[3] P. Allbrecht, J. Appiarius, R. McCoy, and E. Owen, "Assessment of the reliability of motors in utility applications—updated," *IEEE Trans Energy Convers*, pp. 39–46, 1986.

[4] V. V. Thomas, K. Vasudevan, and V. J. Kumar, "Implementation of online air-gap torque monitor for detection of squirrel cage rotor fault using tms320c31," *Int. Conf. on Power Electron., Machi. Drives,*, pp. 128–132, 2002.

[5] P. Vas, *Parameter estimation, condition monitoring and diagnosis of electrical machines*. Oxford: Clarendon Press, Oxford, 1993.

[6] W. Deleroi, "Broken bars in squirrel cage rotor of an induction motor-part i: description by superimposed fault currents," *Arch Elektrotech*, pp. 91–99, 1984.

[7] M. Blodt, P. Granjon, B. Raison, and G. Rostaing, "Models for Bearing Damage Detection in Induction Motors Using Stator Current Monitoring," *IEEE Transactions on Industrial Electronics*, vol. 55, no. 4, pp. 1813–1822, Apr. 2008. [Online]. Available: http://ieeexplore.ieee.org/document/4438690/

[8] M. Benbouzid, M. Vieira, and C. Theys, "Induction motors' faults detection and localization using stator current advanced signal processing techniques," *IEEE Transactions on Power Electronics*, vol. 14, no. 1, pp. 14–22, Jan. 1999. [Online]. Available: https://ieeexplore.ieee.org/document/737588/

[9] M. Seera, Chee Peng Lim, D. Ishak, and H. Singh, "Fault Detection and Diagnosis of Induction Motors Using Motor Current Signature Analysis and a Hybrid FMM–CART Model," *IEEE Transactions on Neural Networks and Learning Systems*, vol. 23, no. 1, pp. 97–108, Jan. 2012. [Online]. Available: http://ieeexplore.ieee.org/document/6104222/

[10] J. Stack, T. Habetler, and R. Harley, "Bearing Fault Detection via Autoregressive Stator Current Modeling," *IEEE Transactions on Industry Applications*, vol. 40, no. 3, pp. 740–747, May 2004. [Online]. Available: http://ieeexplore.ieee.org/document/1300727/

[11] Y. Lei, Z. Qiao, X. Xu, J. Lin, and S. Niu, ""an underdamped stochastic resonance method with stable-state matching for incipient fault diagnosis of rolling element bearings," *Mech. Syst. Signal Process.*, vol. 94, pp. 148–164, 2017.

[12] M. A. Hmida and A. Braham, "An On-Line Condition Monitoring System for Incipient Fault Detection in Double-Cage Induction Motor," *IEEE Transactions on Instrumentation and Measurement*, vol. 67, no. 8, pp. 1850–1858, Aug. 2018. [Online]. Available: https://ieeexplore.ieee.org/document/8306135/

[13] A. Choudhary, D. Goyal, S. L. Shimi, and A. Akula, "Condition Monitoring and Fault Diagnosis of Induction Motors: A Review," *Archives of Computational Methods in Engineering*, vol. 26, no. 4, pp. 1221–1238, Sep. 2019. [Online]. Available: http://link.springer.com/10.1007/s11831-018-9286-z

[14] L. Eren and M. Devaney, "Bearing Damage Detection via Wavelet Packet Decomposition of the Stator Current," *IEEE Transactions on Instrumentation and Measurement*, vol. 53, no. 2, pp. 431–436, Apr. 2004. [Online]. Available: http://ieeexplore.ieee.org/document/1284875/

[15] B. Ayhan, M.-Y. Chow, and M.-H. Song, "Multiple Signature Processing-Based Fault Detection Schemes for Broken Rotor Bar in Induction Motors," *IEEE Transactions on Energy Conversion*, vol. 20, no. 2, pp. 336–343, Jun. 2005. [Online]. Available: http://ieeexplore.ieee.org/document/1432846/

[16] J. Zarei and J. Poshtan, "An advanced Park's vectors approach for bearing fault detection," *Tribology International*, vol. 42, no. 2, pp. 213–219, Feb. 2009. [Online]. Available: https://linkinghub.elsevier.com/retrieve/pii/S0301679X08001291

[17] I. Aydin, M. Karakose, and E. Akin, "A new method for early fault detection and diagnosis of broken rotor bars," *Energy Conversion and Management*, vol. 52, no. 4, pp. 1790–1799, Apr. 2011. [Online]. Available: https://linkinghub.elsevier.com/retrieve/pii/S0196890410005273

[18] J. Pons-Llinares, J. A. Antonino-Daviu, M. Riera-Guasp, S. Bin Lee, T.-j. Kang, and C. Yang, "Advanced Induction Motor Rotor Fault Diagnosis Via Continuous and Discrete Time–Frequency Tools," *IEEE Transactions on Industrial Electronics*, vol. 62, no. 3, pp. 1791–1802, Mar. 2015. [Online]. Available: https://ieeexplore.ieee.org/document/6894134

[19] D. Miljković, "Brief review of motor current signature analysis," *HDKBRINFO Magazin*, vol. 5, pp. 14–26, 2015.

[20] K. D. Kompella, V. G. R. Mannam, and S. R. Rayapudi, "DWT based bearing fault detection in induction motor using noise cancellation," *Journal of Electrical Systems and Information Technology*, vol. 3, no. 3, pp. 411–427, Dec. 2016. [Online]. Available: https://linkinghub.elsevier.com/retrieve/pii/S2314717216300496

[21] J. Zhang, P. Wang, R. X. Gao, C. Sun, and R. Yan, "Induction Motor Condition Monitoring for Sustainable Manufacturing," *Procedia Manufacturing*, vol. 33, pp. 802–809, 2019. [Online]. Available: https://linkinghub.elsevier.com/retrieve/pii/S2351978919305827

[22] O. Janssens, V. Slavkovikj, B. Vervisch, K. Stockman, M. Loccufier, S. Verstockt, R. Van de Walle, and S. Van Hoecke, "Convolutional Neural Network Based Fault Detection for Rotating Machinery," *Journal of Sound and Vibration*, vol. 377, pp. 331–345, Sep. 2016. [Online]. Available: https://linkinghub.elsevier.com/retrieve/pii/S0022460X16301638

[23] A. Duda and P. Drozdowski, "Induction Motor Fault Diagnosis Based on Zero-Sequence Current Analysis," *Energies*, vol. 13, no. 24, p. 6528, Dec. 2020. [Online]. Available: https://www.mdpi.com/1996-1073/13/24/6528

[24] B. Ayhan, M.-Y. Chow, and M.-H. Song, "Multiple Discriminant Analysis and Neural-Network-Based Monolith and Partition

Fault-Detection Schemes for Broken Rotor Bar in Induction Motors," *IEEE Transactions on Industrial Electronics*, vol. 53, no. 4, pp. 1298–1308, Jun. 2006. [Online]. Available: http://ieeexplore.ieee.org/document/1667927/

[25] M. S. Ballal, Z. J. Khan, H. M. Suryawanshi, and R. L. Sonolikar, "Adaptive Neural Fuzzy Inference System for the Detection of Inter-Turn Insulation and Bearing Wear Faults in Induction Motor," *IEEE Transactions on Industrial Electronics*, vol. 54, no. 1, pp. 250–258, Feb. 2007. [Online]. Available: http://ieeexplore.ieee.org/document/4084640/

[26] D. Verstraete, A. Ferrada, E. L. Droguett, V. Meruane, and M. Modarres, "Deep Learning Enabled Fault Diagnosis Using Time-Frequency Image Analysis of Rolling Element Bearings," *Shock and Vibration*, vol. 2017, pp. 1–17, 2017. [Online]. Available: https://www.hindawi.com/journals/sv/2017/5067651/

[27] S. Zolfaghari, S. Noor, M. Rezazadeh Mehrjou, M. Marhaban, and N. Mariun, "Broken Rotor Bar Fault Detection and Classification Using Wavelet Packet Signature Analysis Based on Fourier Transform and Multi-Layer Perceptron Neural Network," *Applied Sciences*, vol. 8, no. 1, p. 25, Dec. 2017. [Online]. Available: http://www.mdpi.com/2076-3417/8/1/25

[28] T. Ince, "Real-time broken rotor bar fault detection and classification by shallow 1D convolutional neural networks," *Electrical Engineering*, vol. 101, no. 2, pp. 599–608, Jun. 2019. [Online]. Available: http://link.springer.com/10.1007/s00202-019-00808-7

[29] M. Valtierra-Rodriguez, J. Amezquita-Sanchez, A. Garcia-Perez, and D. Camarena-Martinez, "Complete Ensemble Empirical Mode Decomposition on FPGA for Condition Monitoring of Broken Bars in Induction Motors," *Mathematics*, vol. 7, no. 9, p. 783, Aug. 2019. [Online]. Available: https://www.mdpi.com/2227-7390/7/9/783

[30] A. Choudhary, D. Goyal, and S. S. Letha, "Infrared Thermography-Based Fault Diagnosis of Induction Motor Bearings Using Machine Learning," *IEEE Sensors Journal*, vol. 21, no. 2, pp. 1727–1734, Jan. 2021. [Online]. Available: https://ieeexplore.ieee.org/document/9165074/

[31] S. K. Gundewar and P. V. Kane, "Condition Monitoring and Fault Diagnosis of Induction Motor," *Journal of Vibration Engineering & Technologies*, vol. 9, no. 4, pp. 643–674, Jun. 2021. [Online]. Available: https://link.springer.com/10.1007/s42417-020-00253-y

[32] M. Kang, J. Kim, J.-M. Kim, A. C. C. Tan, E. Y. Kim, and B.-K. Choi, "Reliable Fault Diagnosis for Low-Speed Bearings Using Individually Trained Support Vector Machines With Kernel Discriminative Feature Analysis," *IEEE Transactions on Power Electronics*, vol. 30, no. 5, pp. 2786–2797, May 2015. [Online]. Available: http://ieeexplore.ieee.org/document/6899683/

[33] R. A. Patel and B. R. Bhalja, "Condition Monitoring and Fault Diagnosis of Induction Motor Using Support Vector Machine," *Electric Power Components and Systems*, vol. 44, no. 6, pp. 683–692, Apr. 2016. [Online]. Available: http://www.tandfonline.com/doi/full/10.1080/15325008.2015.1131762

[34] Sridhar S., K. U. Rao, R. Umesh, and Harish K. S., "Condition monitoring of Induction Motor using statistical processing," in *2016 IEEE Region 10 Conference (TENCON)*. Singapore: IEEE, Nov. 2016, pp. 3006–3009. [Online]. Available: http://ieeexplore.ieee.org/document/7848597/

[35] S. Zgarni, H. Keskes, and A. Braham, "Nested SVDD in DAG SVM for induction motor condition monitoring," *Engineering Applications of Artificial Intelligence*, vol. 71, pp. 210–215, May 2018. [Online]. Available: https://linkinghub.elsevier.com/retrieve/pii/S0952197618300484

[36] M. Benbouzid and G. Kliman, "What stator current processing-based technique to use for induction motor rotor faults diagnosis?" *IEEE Transactions on Energy Conversion*, vol. 18, no. 2, pp. 238–244, Jun. 2003. [Online]. Available: http://ieeexplore.ieee.org/document/1201095/

[37] "Samotics Company, Leiden, 2333 CT, The Netherlands, url = https://www.samotics.com/."

[38] A. T. Johansson, R. K. Lennartsson, E. Nolander, and S. Petrović, "Improved passive acoustic detection of divers in harbor environments using pre-whitening," in *OCEANS 2010 MTS/IEEE SEATTLE*, 2010, pp. 1–6.

[39] A. E. Jaramillo, J. K. Nielsen, and M. G. Christensen, "A study on how pre-whitening influences fundamental frequency estimation," in *ICASSP 2019 - 2019 IEEE International Conference on Acoustics, Speech and Signal Processing (ICASSP)*, 2019, pp. 6495–6499.

[40] H. Ghaderi and P. Kabiri, "Fourier Transform and Correlation-based Feature Selection for Fault Detection of Automobile Engines," p. 6, 2012.

[41] N. V. Chawla, K. W. Bowyer, L. O. Hall, and W. P. Kegelmeyer, "SMOTE: synthetic minority over-sampling technique," *CoRR*, vol. abs/1106.1813, 2011. [Online]. Available: http://arxiv.org/abs/1106.1813

[42] H. He and Y. Ma, *Imbalanced Learning: Foundations, Algorithms, and Applications*, 1st ed. Hoboken, USA: Wiley-IEEE Press, 2013.

[43] J. Kong, W. Kowalczyk, D. A. Nguyen, T. Bäck, and S. Menzel, "Hyperparameter optimisation for improving classification under class imbalance," in *2019 IEEE Symposium Series on Computational Intelligence (SSCI)*, 2019, pp. 3072–3078.

[44] J. Huang and C. X. Ling, "Using auc and accuracy in evaluating learning algorithms," *IEEE Transactions on knowledge and Data Engineering*, vol. 17, no. 3, pp. 299–310, 2005.

[45] V. López, A. Fernández, S. García, V. Palade, and F. Herrera, "An insight into classification with imbalanced data: Empirical results and current trends on using data intrinsic characteristics," *Information sciences*, vol. 250, pp. 113–141, 2013.

[46] C. Jing and J. Hou, "Svm and pca based fault classification approaches for complicated industrial process," *Neurocomputing*, vol. 167, pp. 636 – 642, 2015. [Online]. Available: http://www.sciencedirect.com/science/article/pii/S0925231215004610